



Zaggoulos, G., Tran, M., & Nix, AR. (2008). *Mobile WiMAX system performance – simulated versus experimental results*. 1 - 5.
<https://doi.org/10.1109/PIMRC.2008.4699670>

Peer reviewed version

Link to published version (if available):
[10.1109/PIMRC.2008.4699670](https://doi.org/10.1109/PIMRC.2008.4699670)

[Link to publication record in Explore Bristol Research](#)
PDF-document

University of Bristol - Explore Bristol Research

General rights

This document is made available in accordance with publisher policies. Please cite only the published version using the reference above. Full terms of use are available:
<http://www.bristol.ac.uk/pure/user-guides/explore-bristol-research/ebr-terms/>

Mobile WiMAX System Performance – Simulated versus Experimental Results

George Zaggoulos, Mai Tran and Andrew Nix
Centre for Communications Research, University of Bristol
Bristol, United Kingdom

Abstract- This paper addresses the downlink performance of mobile WiMAX operating at 2.3GHz in an urban environment. The analysis includes a comparison of simulated and experimental results. Simulated packet error rate (PER) versus Signal to Noise Ratio (SNR) graphs are generated on a per link-speed basis using a fully compliant 512 carrier mobile WiMAX simulator. Experimental data is gathered using a carrier-class basestation, a mobile-WiMAX enabled laptop, and a suite of application layer logging software. An H264 AVC encoder and IP packetisation unit is used to transmit video to a mobile client. Results show strong agreement in terms of simulated and captured PER. Using this data, the downlink operating range is evaluated as a function of the Effective Isotropic Radiated Power (EIRP) and path loss exponent. Results indicate that at low EIRP (32 dBm) the expected outdoor operating range is around 200-400m. Applying the UK OFCOM regulations for licensed operation in the 2.5GHz band, downlink operation in excess of 2km can be achieved.

Keywords: Mobile WiMAX, 802.16e, packet error rate

I. INTRODUCTION

WiMAX technology was first standardised in 2002. The initial offering supported fixed wireless broadband connections in metropolitan area networks (MAN) at 10-66 GHz [1]. Later, the standard was extended to cover the 2-11GHz band. In 2004, the draft 802.16 standard was published as 802.16-2004 [2]. This update focused on providing better support for fixed and nomadic applications. It introduced two new physical layer (PHY) technologies: 1) Orthogonal frequency division multiplexing (OFDM) with 256 sub-carriers and 2) OFDMA with up to 2048 sub-carriers. Within the 802.16-2004 standards a limited degree of mobility is permitted. Movement results in a Doppler shift, which for a given multipath component (MPC) is proportional to the carrier frequency and the relative velocity between the basestation and terminal. In a multipath environment, each individual MPC experiences a unique Doppler shift; thus creating a Doppler spread [3]. Unless the temporal envelope variations that result from Doppler spread are successfully mitigated on a per sub-carrier basis, this will result in an irreducible bit error rate (i.e. an error rate that cannot be reduced by increasing the SNR).

In 2005, the IEEE 802.16e working group produced a further amendment to allow enhanced mobility and support for handover. The 802.16e standard has been developed for mobile speeds up to 120 km/h at 3.8 GHz [4]. Mobile WiMAX supports multiple-access using scalable OFDMA. Data streams to and from individual users are multiplexed to groups of sub-channels on the downlink and uplink. By

adopting a scalable PHY architecture, mobile WiMAX is able to support a wide range of bandwidths, as shown in Table 1. The scalability is implemented by varying the FFT size from 128 to 512, 1024, and 2048 to support channel bandwidths of 1.25 MHz, 5 MHz, 10 MHz, and 20 MHz respectively. For mobile applications, where the channel varies rapidly in time, the continuous use of high spectral efficiency schemes, such as 64QAM, is difficult to achieve. To overcome this limitation adaptive modulation and coding (AMC) is employed to dynamically select the best modulation scheme given knowledge of the radio channel. Consequently, on a per-link basis, this maintains the highest possible bandwidth efficiency under all operating conditions.

The rest of the paper is organized as follows: The experimental configuration, including the parameters used, is described in section II. The mobile WiMAX simulator and channel model is described in section III. Experimental results are presented in section IV, compared with our earlier simulations. Finally, conclusions are drawn in section V.

II. EXPERIMENTAL CONFIGURATION

Measurements were performed using a mobile terminal (MT) connected to a commercial carrier-class WiMAX basestation (BS). The BS used time division duplex (TDD) with scheduling based on a Round-Robin technique. The PHY layer used 1024 sub-carriers in a 10 MHz bandwidth. The ratio between the downlink and uplink was 80:20 in favour of the downlink. Table 2 summarizes the key parameters for the equipment used. The BS power amplifier was connected via 30m of RF cable to a 2 dBi dipole antenna. This was mounted on the roof of a two-storey building. An EIRP of 32dBm was assumed at the BS.

Table 1: WiMAX OFDMA PHY Parameters

Parameter	Value			
FFT size	128	512	1024	2048
Channel bandwidth (MHz)	1.25	5	10	20
Subcarrier spacing (kHz)	10.94			
Useful symbol period (μs)	91.4			
Guard Time	1/32, 1/16, 1/8, 1/4			

Table 2: WiMAX Base Station Parameters

Parameter	Value
Operating Frequency	2.3 GHz
Bandwidth	10 MHz
FFT Size	1024 (Partial Use of Sub-Carriers)
BS Antenna Gain	2 dBi (dipole)
Mean basestation Tx Power	40 dBm

The MT comprised a laptop computer using an 802.16e compatible PC-card. Two identical laptops were placed in a vehicle to transmit and receive data. At the application layer the IP data packets were sent in broadcast mode (i.e. no application layer acknowledgement or retransmission was used to enhance the link quality). The vehicle was driven in the BS coverage area at speeds up to 35 km/h. The route involved passing through the radio shadow of numerous tall buildings. The experiment included the logging of PER, data throughput and signal level in addition to GPS location (to determine the BS-MT separation distance).

Two experimental configurations were used. The first employed client-server logging software developed jointly between the University of Bristol and ProVision Communications. This server generates unicast and broadcast traffic while the client records throughput, mean delay and jitter, PER, GPS data (location and time) and vehicle speed. The software is also able to record RSSI and link-speed if supported at the driver level. Our use of pre-release mobile WiMAX PC cards prevented the logging of these last two parameters. Apart from the GPS data, which was recorded as a snapshot every second, all the other parameters were recorded as a per-second average. Hence, the impact of fast-fading was averaged to yield an estimate of the local mean power [5]. The server was connected via Ethernet directly to the BS, while the client was installed in the vehicle.

The second configuration was based on the ProVu video server. This unit, developed by ProVision Communications, takes in audio and composite video and converts them into a standard IP stream (at a programmable data rate). Video compression is performed using the H264 AVC standard. The integrated IP server adds additional information to enable the software client to log PER and throughput on a per-second basis. The client is also able to decode the incoming IP stream and display (or save) the resulting video.

The first experimental approach was mainly used for PER and throughput testing, while the second method was preferred when testing the broadcast capability of the WiMAX network.

Given the difficulties of RSSI acquisition using our specific WiMAX PC-card, it was decided to operate in parallel an 802.11g network. This consisted of a second ProVu server connected via Ethernet to a WiFi access point (AP). This was placed close to the WiMAX dipole antenna. A second laptop with a WiFi PC-card was placed in the vehicle. The RSSI of the WiFi AP was recorded on this second laptop together with GPS location and time. The recorded RSSI from the 802.11g network was used to compute the path loss, which was then used in the WiMAX analysis. This approach is acceptable since the WiMAX and WiFi networks operate at 2.3 and 2.4GHz respectively, and only the local mean RSSI was recorded. The path loss exponent was extracted from the experimental data using Erceg's empirically based model [5]. This can be written as

$$PL = A + 10\gamma \text{Log}_{10}(d/d_o) + s; \quad d \geq d_o \quad (1)$$

where γ represents the path loss exponent and d and d_o are the BS-MT separation and reference distances respectively. S is used to represent the shadow fading and A denotes a fixed

quantity that is given by the free-space path loss formula [6].

$$A = 20\text{Log}_{10}(4\pi d_o / \lambda) \quad (2)$$

where λ denotes the carrier wavelength. In our analysis the reference distance d_o is set to 1m.

The propagation environment around the BS consists mainly of large office and industrial buildings (with heights ranging from 5m to 30m). Several housing developments and a number of open fields can be seen further away from the BS. The BS antenna is located at the centre of the circles shown in Figure 1. This location was chosen due to its close proximity to the rack of BS equipment. The location is far from optimum, since it is surrounded by high buildings and is close to a number of tall trees (which introduces severe shadowing). Unfortunately, it was not possible to relocate the BS, and hence the resulting coverage is less than that expected for a professional deployment. The bulk of our measurements were taken in challenging non-LoS conditions, with an observed path loss exponent between 2.3 and 3.5. Analytical information on the characteristics of the propagation environment is provided in section IV.

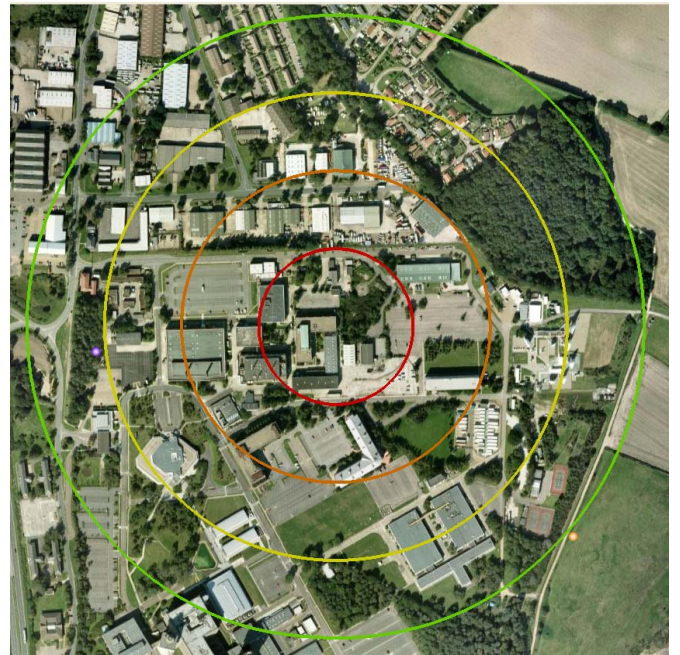


Figure 1: Trial Location (circles plotted every 100 m from BS)

III. SIMULATION CONFIGURATION

The experimental results reported in this paper are compared with simulated data produced from our mobile WiMAX PHY layer simulator. The simulator is designed to be compliant with the 802.16e-2005 standard. The parameters used in the simulation study are listed in Tables 3 and 4.

The channel model is based on the ETSI 3GPP-3GPP2 spatial channel model (SCM) [7]. This model was developed to help standardise the outdoor evaluation of mobile systems. The 3GPP SCM defines three typical cellular environments, namely urban macrocell (cell radius less than 1.5 km, BS antenna well above rooftop level), suburban macrocell (cell

radius less than 1.5km, BS antenna well above local cluster), and urban microcell (cell radius less than 500 meters, BS antenna at rooftop level).

Table 3: WiMAX simulator parameters

Parameter	Value
Operating Frequency	2.3 GHz
Channel Bandwidth	5 MHz
Sampling Frequency	5.6 MHz
FFT Size	512
Number of Used Sub-carriers	421
Sub-carrier Spacing $\Delta f = F_s / N_{FFT}$	10.94 kHz
Sampling Period	0.18 μ s
Useful Symbol Duration $T_b = 1 / \Delta f$	91.4 μ s
Guard Interval Length $T_g = T_b / 8$	11.4 μ s
OFDMA Symbol Duration $T_s = T_b + T_g$	102.9 μ s
Number of Sub-channels	15
Number of Users	3
Number of Sub-channels/User	5
Number of Data Sub-carriers	360

Using the 3GPP-SCM channel model, an urban micro tapped delay line (TDL) is generated to represent the wideband channel. This model consists of 6 non-uniform delay taps. The MT velocity is set to 40 km/h, which is just above the maximum value used in the trials. The channel parameters are summarized in Table 4.

Table 4: Channel parameters

	Tap 1	Tap 2	Tap 3	Tap 4	Tap 5	Tap 6
Delay (ns)	0	210	470	760	845	910
Power (dB)	0	-1.8	-1.5	-7.2	-10	-13
K factor	0	0	0	0	0	0
Delay spread	279 ns					

The packet structure follows the latest published amendment [8] of the mobile WiMAX standard. It consists of n (variable) OFDMA symbols, with the value depending on the chosen modulation and coding mode (i.e. the link-speed). The first symbol in each packet, as shown in Figure 2, is a preamble, with the remaining (variable number of) symbols containing the payload data.

Preamble	Data 1	Data 2	...	Data n
----------	--------	--------	-----	--------

Figure 2: Mobile WiMAX packet structure

Each packet is a self-contained entity. In our simulations the receiver assumes perfect synchronisation and ideal channel estimation. As a result, a degradation of 1-2 dB should be allowed for practical hardware.

Table 5 lists the link-speeds available on the downlink of mobile WiMAX. The maximum data rate per user is also given based on the assumption that each user is allocated 120 sub-carriers in an OFDMA symbol. In practice, higher data rates can be supported if more subcarriers are allocated to the user.

Table 5: WiMAX DL Link-Speeds (120 sub-carriers/user)

Mode (Modulation & Code Rate)	WiMAX Downlink Link-Speed/user (Mbps)
QPSK 1/2	1.17
QPSK 3/4	1.75
16 QAM 1/2	2.33
16 QAM 3/4	3.50
64 QAM 1/2	3.50
64 QAM 2/3	4.66
64 QAM 3/4	5.25

IV. RESULTS

The experimental results presented in this paper are based on the downlink PER performance for a 256 kbps video stream. This stream was broadcasted as a sequence of IP packets from a ProVu unit (see Section II). The PER was recorded at the ProVu client, while the path loss exponent (and the derived SNR) was estimated using Erceg's path loss model. The path loss exponent (for the local area) was derived using RSSI levels extracted from a parallel WiFi network.

The downlink PER performance is based on 2500 data samples collected at the MT while driving in the vicinity of the BS. In all cases the MT received a broadcasted video stream over the WiMAX link. Figures 3-6 provide an insight into the environment (including path loss exponents, distances from the BS and the distribution of measured SNR). The routes followed are shown in figure 3 together with spot estimates of the local path loss exponent. Figure 4 shows the distribution of the distance from the BS where measurements were recorded, while figure 5 presents the distribution of the path loss exponent. Finally, figure 6 shows the distribution of the estimated SNR. The number on top of each column represents the number of recorded data samples.

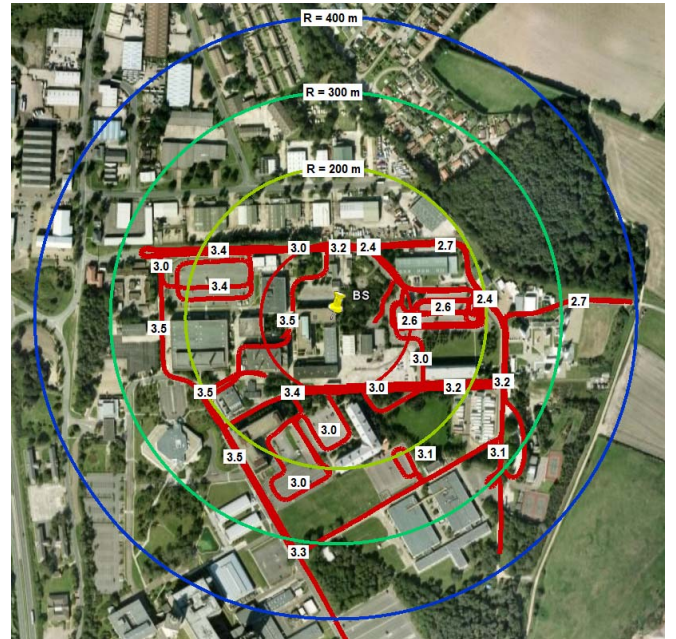


Figure 3: Routes followed during the trials with spot estimates of the resulting path loss exponent.

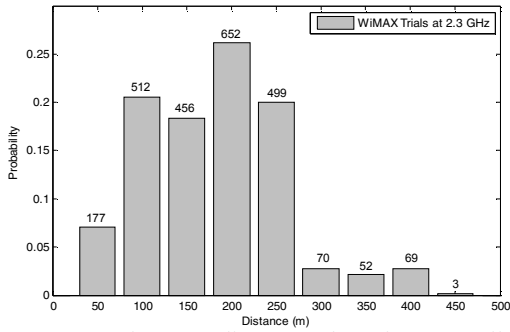


Figure 4: PDF of BS-MT distances where data was collected

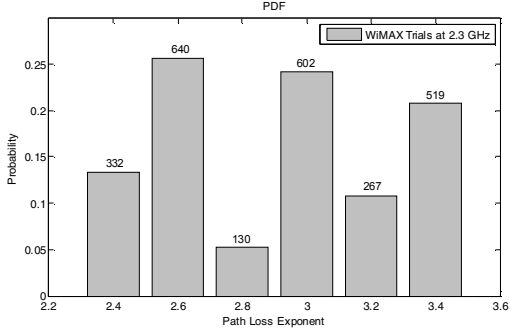


Figure 5: PDF of Estimated Path loss Exponent

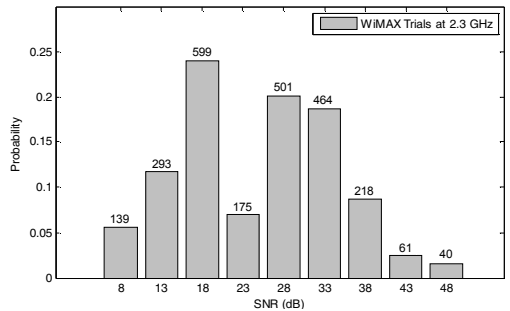


Figure 6: PDF of Estimated SNR

The routes used in this experiment were carefully chosen to cover a wide range of different locations, whilst ensuring that the vehicle remained within the cell boundary. From figure 4 it can be seen that the longest BS-MT separation distance is 450m. The cell radius is much less than that commonly expected for mobile WiMAX. This can be explained as follows. The BS EIRP in this experiment was approximately 32 dBm. This low value can be attributed to cable loss and the use of a dipole antenna. If a high-gain sectorised antenna had been used, the EIRP could have been increased by 16dB. In the UK, operation in the licensed 2GHz band is regulated by OFCOM. The permitted EIRP for a 10MHz signal is 61 dBm. Assuming the BS is able to supply this level of power to the antenna port, use of the maximum regulated power level will significantly increase the downlink range (see later analysis). Range was also reduced by the low mounting of the BS antenna, and the surround high-level buildings and trees. The poor location of the BS is partly responsible for the high path loss exponents. This is compounded by the non-line-of-sight location of the vehicle, which regularly passed through areas of high shadow loss.

The PER versus SNR performance seen in this experiment is not significantly affected by the poor BS location and low EIRP. Figure 6 shows the PDF of the estimated SNR values,

which lie in a range from 8dB to 48dB. As a result of power control, the higher SNR values would not be seen in practice. From the 2500 recorded data samples (one every second), most are observed to lie between 16-20dB and 26-35dB. A relatively small number of data samples were captured at the extremes of the SNR range.

The downlink PER performance of the mobile WiMAX BS is presented in figure 7 together with our simulated results using the models described in section III. As a result of link adaptation, each link-speed is used over a narrow range of SNR values. This range is quoted from the mobile WiMAX standard [8] in the legend of figure 7. Using the estimated SNR for each measurement, we use these link adaptation ranges to choose the selected link-speed. Once the link-speed has been determined, we can then compare the measured result with our theoretic data. For example, a measured SNR of 13dB would use the 16QAM $\frac{3}{4}$ rate mode.

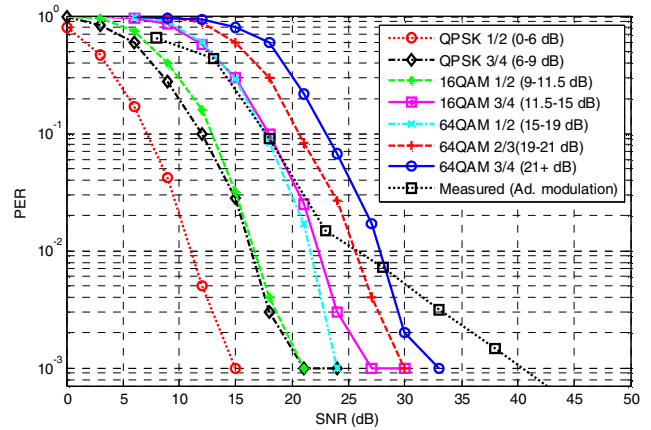


Figure 7: PER comparison

It is clear from the above comparison that a good agreement exists between the measured and simulated data. The greatest discrepancy occurs for the highest SNR values. These values are estimated without considering the impact of power control. In practice, for SNR values beyond 21dB the BS will lower the transmit power, thus reducing the observed SNR.

Figure 8 shows the measured PER and estimated RSSI as a function of elapsed time (PER < 0.001 is plotted as 10^{-3}). To aid discussion, we assume a maximum PER of 10^{-1} (beyond this value we assume the system is in outage). By calculating the CDF of the PER, the system outage from the measured data is approximately 12%. It is clear that PER values greater than 10^{-1} occur when the estimated RSSI level is less than or equal to -80 dBm. According to the mobile WiMAX standard, the sensitivity of a MT is around -82 dBm. Given the early release nature of the hardware under test, this also agrees well with our experimental data.

Having demonstrated the required RF sensitivity at the MT, it is clear that the limited downlink operating range is a result of the low EIRP and the poor location of the BS. It is reasonable to expect that the operating range and the measured PER vs BS-MT separation distance could be improved significantly by increasing the BS antenna height [9] and EIRP. As mentioned previously, in the licensed 2.5GHz band OFCOM allows up to 61dBm of EIRP. If we use this maximum EIRP in our link budget, we can compute the expected range for a full power device. The results are shown in figure 9.

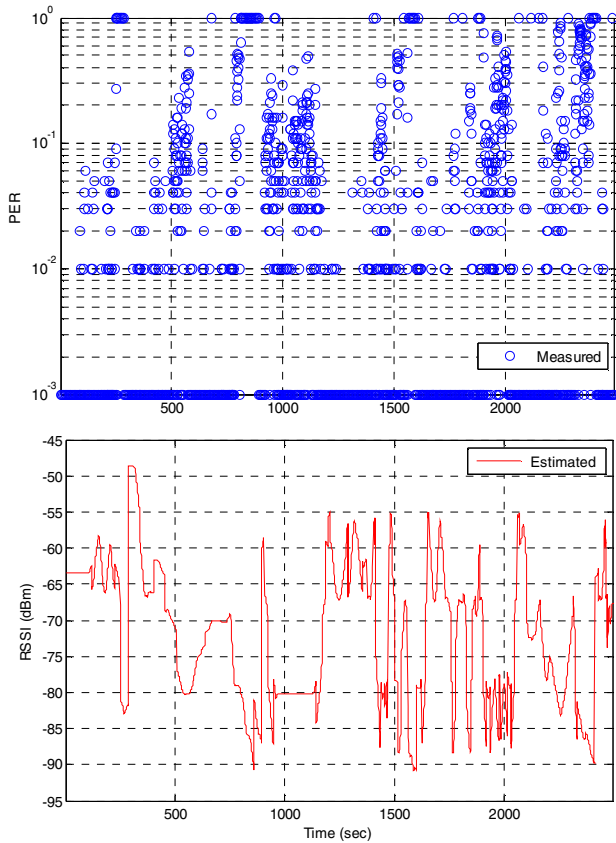


Figure 8: Measured PER (top) and estimated RSSI (bottom) versus Time

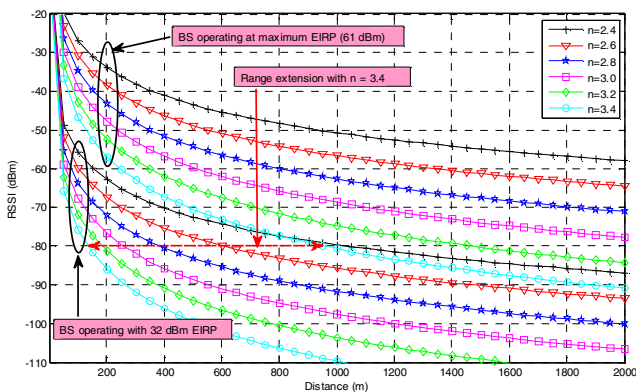


Figure 9: Estimated RSSI versus Distance as a function of Path Loss Exponent and BS EIRP

Two set of graphs are shown in the above figure, one for an EIRP of 32dBm (corresponding to the actual measurements reported here), and another for an EIRP of 61dBm (corresponding to the OFCOM maximum). If we apply the highest path loss exponent seen in our measurement (see figure 5), i.e. $n=3.4$, we see the downlink range increases from 150m to 950m. For $n=2.8$, we see the operating range increases from 400m to well over 2km. It is clear that at high EIRP values the mobile WiMAX standard is capable of achieving a high level of outdoor NLoS coverage. To achieve the high EIRP levels required, high-gain sectorised antennas are desirable. If we assume a sectorised antenna gain of 18dBi, to reach the OFCOM peak a mean power level of 43dBm (20 Watts) is required. Allowing for the typical peak-to-mean-power ratio (PMPR) of OFDMA, the peak power rating of each power amplifier needs to be 100-200 Watts.

Although this power level is achievable in carrier-class equipment (such as the BS under trial here), it is not currently available in the majority of proposed WiMAX BS.

V. CONCLUSIONS

This paper has analysed the downlink performance of mobile WiMAX using a combination of simulation and experimentation. A fully compliant mobile WiMAX simulator was used to derive a theoretic set of PER versus SNR graphs. The real-world performance of a WiMAX BS was evaluated by measuring the PER via a number of drive tests. Good agreement was demonstrated between the measured and simulated PER. Using recorded RSSI values, the path loss exponent was estimated for various locations in the cell. By combining the measured path loss estimates with the OFCOM regulations in the licensed 2.5GHz band, the expected performance of a carrier-class mobile WiMAX network was shown to exceed 2km.

ACKNOWLEDGMENTS

This work was partly funded by the Technology Strategy Board (TSB) under the VISUALISE project. The authors would like to thank Dr. James Chung How (ProVision Communications Ltd), Dr. Pierre Ferre and David Halls for their key contributions to the measurement exercise.

REFERENCES

- [1] IEEE, "IEEE Std 802.16-2001," 2002.
- [2] IEEE, "IEEE Std 802.16-2004 (Revision of IEEE Std 802.16-2001)," 2004.
- [3] G. Zaggoulos, A.R. Nix, and A. Doufexi, "WiMAX System Performance in Highly Mobile Scenarios with Directional Antennas," presented at IEEE 18th International Symposium on Personal, Indoor and Mobile Radio Communications (PIMRC'07), Athens, Greece, 2007.
- [4] WiMAX Forum, "Fixed, nomadic, portable and mobile applications for 802.16-2004 and 802.16e WiMAX networks," November 2005.
- [5] V. Erceg, L. Greenstein, S. Tjandra, S. Parkoff, A. Gupta, B. Kulic, A. Julius, and R. Bianchi, "An Empirically Based Path Loss Model for Wireless Channels in Suburban Environments," IEEE Journal on Selected Areas in Communications, vol. 17, pp. 1205-1211, 1999.
- [6] J. D. Parsons, The Mobile Radio Propagation Channel, 2nd ed: Wiley, 2000.
- [7] 3GPP, "Spatial channel model for Multiple Input Multiple Output (MIMO) simulations", TR 25.996 v6.1.0, 2003.
- [8] IEEE, "IEEE Std 802.16e-2005 and IEEE Std 802.16-2004/Cor 1-2005 (Amendment and Corrigendum to IEEE Std 802.16-2004)," 2005.
- [9] M. J. Feuerstein, K. L. Blackard, T. S. Rappaport, S. Y. Seidel, and H. H. Xia, "Path loss, delay spread, and outage models as functions of antenna height for microcellular system design," Vehicular Technology, IEEE Transactions on, vol. 43, pp. 487 - 498 1994.